

Methods for the Optimal Design of Grid-Connected PV Inverters

Eftichios Koutroulis*, Frede Blaabjerg**

* Department of Electronic & Computer Engineering, Technical University of Crete, Greece

** Department of Energy Technology, Aalborg University, Denmark

‡Corresponding Author; Tel: +30 28210 37233, Fax: +30 28210 37542, e-mail: efkout@electronics.tuc.gr, fbl@et.aau.dk

Invited Paper

Abstract- The DC/AC inverters are used in grid-connected PV energy production systems as the power processing interface between the PV energy source and the electric grid. The energy injected into the electric grid by the PV installation depends on the amount of power extracted from the PV power source and the efficient processing of this power by the DC/AC inverter. In this paper two new methods are presented for the optimal design of a PV inverter power section, output filter and MPPT control strategy. The influences of the electric grid regulations and standards as well as the PV array operational characteristics on the design of grid-connected PV inverters have been considered. The proposed methods have been applied for the optimal design of PV inverters installed at various sites in Europe. The simulation results verify that the proposed optimization techniques enable the maximization of the PV energy injected into the electric grid, thus serving as a tool to gain more energy by the optimized PV installation.

Keywords- Photovoltaic power systems; DC-AC power conversion; Design methodology; Optimization methods.

1. Introduction

The DC/AC inverters are used in grid-connected Photovoltaic (PV) energy production systems as the power processing interface between the PV power source and the electric grid. Compared to the grid-connected PV inverters that have galvanic isolation (either on the DC, or the AC side), the transformerless PV inverters have the advantages of lower cost, higher efficiency, smaller size and lower weight [1]. The galvanic isolation provides enhanced safety features, but the necessity for its implementation depends on the electric grid codes imposed by the utility companies in each country [2].

The general block diagram of a grid-connected PV system is illustrated in Fig. 1. The power section of the DC/AC inverter consists of power switches controlled by a control unit. The H-bridge, single-phase with DC decoupling, Refu Solar, H5, HERIC, NPC, Conergy, H-bridge zero vector rectifier, three-phase full-bridge and full-bridge with split capacitor topologies are widely

applied in order to built the power section of transformerless PV inverters since they obtain the highest efficiency [1, 3-5]. In order to increase the PV inverter power density, LCL-type output filters are usually used instead of the L- or LC-type filters [6]. The control unit is usually developed using DSP and FPGA ICs [7, 8] for the execution of control and energy management algorithms (e.g. Maximum Power Point Tracking-MPPT [9], detection of islanding conditions, modulation strategies etc.).

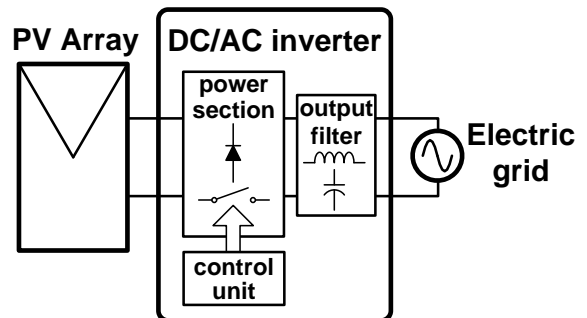


Fig. 1. The block diagram of a grid-connected PV system.

The PWM schemes used to control the power switches of transformerless PV inverters are typically based on the comparison of a low-frequency reference sine-wave with a high-frequency triangular wave [10].

Targeting at the minimization of the power switches losses (conduction and switching) and the equal distribution of these losses among the power switches, or the minimization of the output voltage Total Harmonic Distortion (THD), various PWM Strategies for NPC and Active NPC inverters are investigated in [10-13].

Various international standards (IEEE 1547, EN50160 etc.) set limitations on parameters such as the Total Demand Distortion (TDD %) of the current injected at the PCC and the corresponding limits of the individual harmonics, the maximum values of the voltage harmonic distortion, voltage unbalance, voltage amplitude variations and frequency variations and the maximum permitted DC current injection. These limitations must be considered during the design of PV inverters [6, 14].

Metrics such as the power conversion efficiency and the “European efficiency” are used to evaluate the performance of the designed PV inverter [1, 3]. The PV inverter operating efficiency depends on the power section topology and the type and operational characteristics (conducting and switching) of the components (semiconductors, magnetic elements and capacitors), which are used to build the PV inverter [1, 4]. Typically, the PV inverter efficiency is reduced by 0.3%-1% per 150 V of DC input voltage amplitude. Additionally, it drops by up to 5% at light load and high DC input voltage [15], due to the domination of the control unit and switching power losses during these operating conditions. Currently, the state-of-the-art transformerless PV inverters have maximum power conversion efficiency and European efficiency values (at the nominal DC input voltage) in the order of 98% and 97%, respectively.

The PV inverters are typically designed to operate over a wide DC input voltage range (e.g. 350V-750V) in order to perform the PV array MPPT process under the continuously varying solar irradiation and ambient temperature. The power injected into the grid, the PV inverter power loss and the PV inverter efficiency under MPPT conditions, during the same summer day for a commercial PV inverter installed in Athens (Greece), Murcia (Spain) and Freiburg (Germany), respectively, are plotted in Fig. 2. The corresponding power conversion efficiency of the PV inverter during the same day is illustrated in Fig. 3.

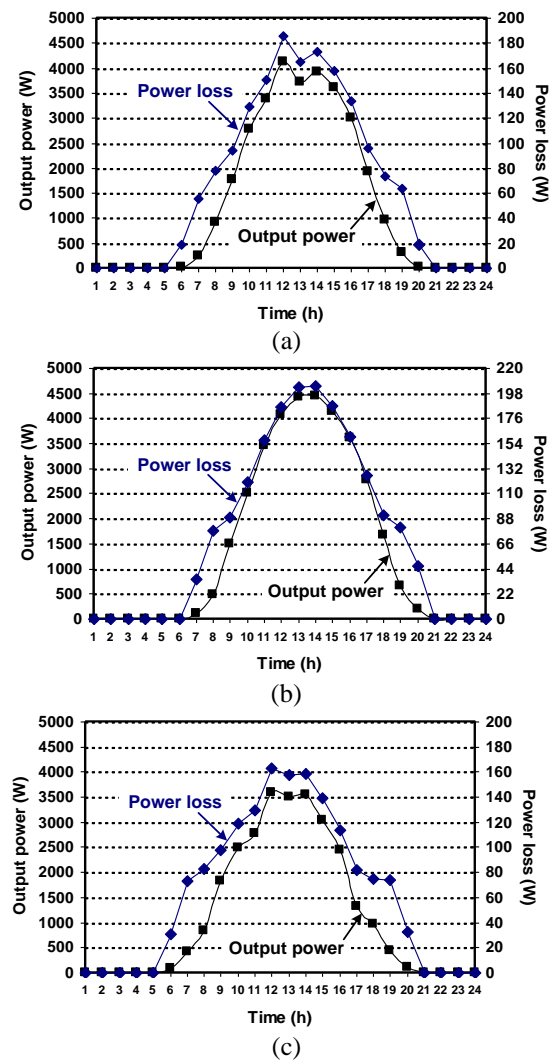


Fig. 2. The output power and power loss variations under MPPT conditions, during the same summer day for a commercially available PV inverter installed in: (a) Athens (Greece), (b) Murcia (Spain) and (c) Freiburg (Germany).

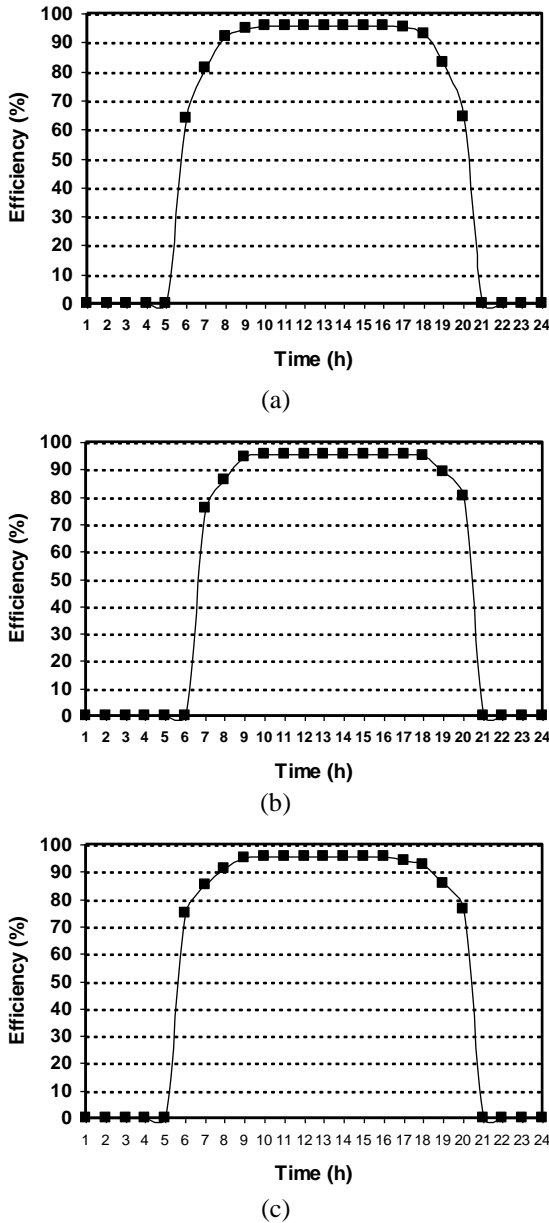


Fig. 3. The variation of the power conversion efficiency under MPPT conditions, during the same summer day for a commercially available PV inverter installed in: (a) Athens (Greece), (b) Murcia (Spain) and (c) Freiburg (Germany).

It is observed that in all cases considered, both the power injected into the grid and the PV inverter power loss vary significantly during the day, although the corresponding power conversion efficiency of the PV inverter remains relatively constant. The stochastically varying meteorological conditions prevailing at the PV array installation site and the effectiveness of the MPPT control strategy performed by the PV

inverter control unit define the amount of power extracted from the PV power source. The actual energy injected into the electric grid depends on the efficient processing of this power by the PV inverter, according to the shape of the PV inverter efficiency vs. output power curve.

The objective of a power converter design optimization procedure is, given the converter topology, to calculate the converter component types, values and dimensions, which result in the minimization (or maximization, depending on its nature) of a certain converter characteristic defined by the designer (e.g. power loss, power density etc.), while simultaneously the performance specifications are met [16, 17]. Using these techniques, power density increments by a factor of 2-4 [18], reduction of the packaged power converter volume by 38.3% [19] and efficiency improvements in the order of 8-20% in the light to medium load region [20] have been achieved. However, none of these methods has yet been applied for the design optimization of PV inverters.

In this paper, two new design optimization methods of PV inverters are presented, for the optimal design of the PV inverter power section, output filter and MPPT control strategy, respectively. The proposed techniques target to exploit the potential of nonlinear optimization methods using multiple decision variables together with linear and nonlinear constraints, for the design of PV inverters. The optimization objective is to maximize the energy injected into the electric grid by the PV inverter, with the minimum possible PV inverter construction and maintenance costs during its lifetime operation. This issue is explored for the first time in the existing literature. The proposed techniques encompass the influences of the electric grid regulations and standards as well as the PV array operational characteristics on the design of grid-connected PV inverters.

The proposed design optimization methods of PV inverters are analyzed in Section 2, while PV inverter design examples using these methods are presented in Section 3.

2. The proposed design optimization methods of PV inverters

2.1. Power section and output filter

A flow-chart of the proposed automated optimization procedure is illustrated in Fig. 4. The optimization algorithm inputs are the following:

- operational characteristics (e.g. power rating, open-circuit voltage etc.) of the PV modules and their configuration in the PV array (e.g. tilt angle, number of modules connected in series etc.),
- 1-min or 1-hour average solar irradiance and ambient temperature time-series during the year,
- input/output voltage ranges and the power rating specifications of the PV inverter,
- PV inverter topology and modulation strategy,

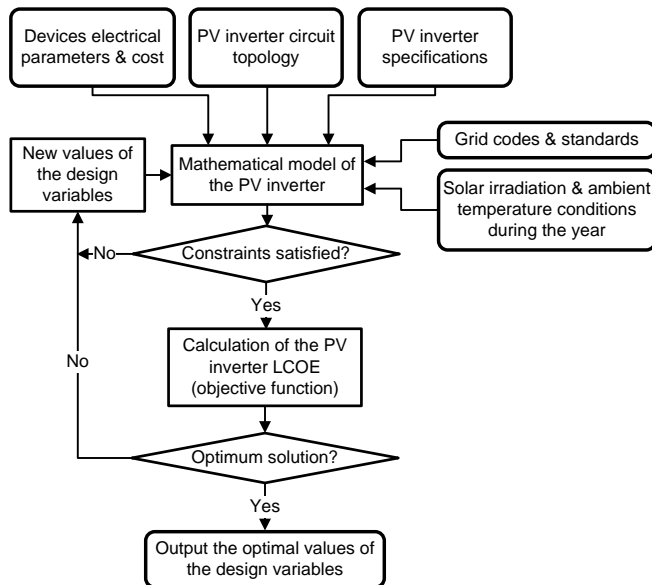


Fig. 4. The flow-chart of the proposed optimization procedure.

- price and device-specific characteristics available in the device datasheet, which define the switching and conducting behaviour of the power semiconductors used to built the inverter,
- price and technical characteristics of commercially available magnetic components and capacitors (in the format

available in the device datasheet) for the construction of the output filter,

- grid-interconnection specifications (e.g. the maximum permitted harmonic current levels etc.) imposed by grid codes and international standards,
- economic parameters (e.g. annual inflation rate etc.).

The proposed design optimization algorithm calculates the optimal values of the following design (decision) variables:

- switching frequency,
- power semiconductors type and configuration (e.g. the number of power MOSFETS connected in parallel),
- power switches gate-drive design parameters, such as the gate series resistances during turn-on and turn-off and the gate-drive supply voltage,
- output filter inductance and capacitance values (depending on the filter type),
- output filter inductor magnetic core size (center-leg width and window width), flux density, current density, copper size and number of turns,
- heat sink dimensions and thermal resistance to the ambient.

Given the PV inverter specifications and the available components electric, magnetic and thermal characteristics, the objective function minimization process is performed by iteratively producing new sets of the design variables values and evaluating the objective function, until convergence to the optimum solution is detected. This procedure is performed using Genetic Algorithms, which are capable to derive the global optimum solution of the objective function with relative computational simplicity. For each set of the design variables values, the satisfaction of the PV inverter operational constraints is verified using the appropriate mathematical models of the PV inverter topology under consideration.

The optimal values of the design variables are calculated such that the PV inverter Levelized

Cost Of the Electricity generated, $LCOE$ (€/Wh), is minimized:

$$\underset{\mathbf{X}}{\text{minimize}} \{LCOE(\mathbf{X})\} = \underset{\mathbf{X}}{\text{minimize}} \left\{ \frac{C_t(\mathbf{X})}{E_t(\mathbf{X})} \right\} \quad (1)$$

subject to:

design specifications & constraints are met

where C_t (€) is the PV inverter total cost during its operational lifetime period, E_t (Wh) is the total energy which is injected into the electric grid by the PV inverter during its operational lifetime period and \mathbf{X} is the vector of the design variables described above. The $LCOE$ minimization process is performed subject to the constraints imposed by the PV inverter specifications and the grid codes and international standards. The $LCOE$ objective function targets to maximize the PV inverter output energy by minimizing the PV inverter total energy losses arising due to the power losses of the PV inverter components, while simultaneously the minimum PV inverter cost is achieved. The $LCOE$ is used as a metric in order to compare the relative cost of electricity among alternative electric energy production solutions [21].

The total energy which is injected into the electric grid by the PV inverter during its operational lifetime period, E_t (Wh), is calculated as follows:

$$E_t = \sum_{y=1}^n \sum_{t=1}^{8760} P_o(t, y) \cdot \Delta t \quad (2)$$

where n (years) is the PV inverter operational lifetime period, $P_o(t, y)$ (W) is the power injected into the grid by the PV inverter at hour t ($1 \leq t \leq 8760$) of year $1 \leq y \leq n$ and Δt is the simulation time-step set to $\Delta t = 1$ hour.

The types and values of the PV inverter components determine the PV inverter reliability characteristics and affect the PV inverter maintenance cost and total energy production during its lifetime period. Thus, in the proposed methodology, the PV inverter failure and repair

rates are calculated for each set of the design variables values, \mathbf{X} , according to the analysis presented in [22]. Then, the power injected into the grid by the PV inverter at hour t ($1 \leq t \leq 8760$) of year $1 \leq y \leq n$ is calculated from the power-balance equation as follows:

$$P_o(t, y) = \begin{cases} 0 & \text{, during repair} \\ P_{pv,t} - P_{tot,t} & \text{, else} \end{cases} \quad (3)$$

where $P_{pv,t}$ (W) is the PV array output power at hour t , which is also equal to the PV inverter input power and $P_{tot,t}$ is the PV inverter total power loss at hour t .

In order to calculate the PV array output power, $P_{pv,t}$, it is assumed that an MPPT process is performed by the PV inverter control unit, such that the maximum PV power is supplied to the PV inverter. The value of $P_{pv,t}$ is calculated using the PV modules model analyzed in [23], based on the solar irradiation and ambient temperature time-series, the electrical specifications of the PV modules and their configuration (i.e. connection in series and parallel) within the PV array, which are input in the proposed optimization procedure by the PV inverter designer. The PV inverter total power loss, $P_{tot,t}$ (W), is equal to the sum of the power switches conduction and switching losses, P_{cond} (W) and P_{sw} (W), respectively, the power loss on the output filter, P_d (W) and the control unit power consumption (due to the circuits of the SPWM modulator, IGBT drivers, sensors and signal conditioners etc.), P_{cu} (W):

$$P_{tot,t} = P_{cond} + P_{sw} + P_d + P_{cu} \quad (4)$$

The PV inverter total cost, C_t (€), is calculated as the sum of the manufacturing cost and the maintenance cost during its operational lifetime period. The PV inverter total manufacturing cost is equal to the sum of the prices of the components comprising the PV inverter. The maintenance cost is estimated based on the PV inverter failure rate, which is calculated

by performing the reliability analysis described above.

2.2. Control strategy

The control unit of the PV inverter performs an MPPT function continuously in order to maximize the energy generated by the PV array. The MPPT schemes applied are based on the attributes of the PV array current-voltage characteristic. This leads to PV inverter operation at variable DC input voltage and power levels, depending on the solar irradiation and ambient temperature conditions. The PV inverter efficiency, n_{inv} (%), varies accordingly:

$$n_{inv} = \frac{P_{grid}}{P_{pv}} = g(P_{pv}, V_{pv}) = g(f(V_{pv}, G, T_A), V_{pv}) \quad (5)$$

where P_{grid} (W) is the PV inverter output power, P_{pv} (W) and V_{pv} (V) are the PV array output power and voltage, respectively, G (W/m^2) is the solar irradiance and T_A ($^{\circ}C$) is the ambient temperature. Thus, the PV inverter output power, which is injected to the electric grid, is calculated as follows:

$$\begin{aligned} P_{grid} &= g(f(V_{pv}, G, T_A), V_{pv}) \cdot P_{pv} \\ &= g(f(V_{pv}, G, T_A), V_{pv}) \cdot f(V_{pv}, G, T_A) \\ &= h(V_{pv}, G, T_A) \end{aligned} \quad (6)$$

It is observed that the power injected into the electric grid depends on the PV array output voltage, the solar irradiance and the ambient temperature. The application of a conventional MPPT scheme [9] on the PV array power-voltage characteristic depicted in Fig. 5, results in the PV array operation at point A. However, due to the PV inverter power conversion efficiency characteristics, the power injected by the PV inverter into the electric grid is maximized at point B. In order to operate the PV array under the stochastically varying meteorological conditions, at the point where the power injected into the electric grid is maximized (i.e. point B in Fig. 5), the MPPT process implemented in the control unit

of the PV inverter [24] can be performed using a ‘‘Perturb & Observe’’ algorithm, according to the following control law:

$$c_{s,k} = c_{s,k-1} + \Delta c_{s,k-1} \quad (7)$$

$$\Delta c_{s,k-1} = C \cdot \text{sign}(\Delta c_{s,k-2}) \cdot \text{sign}\left(\frac{P_{grid,k-1} - P_{grid,k-2}}{V_{pv,k-1} - V_{pv,k-2}}\right)$$

where $\Delta c_{s,k-1}$ is the control signal (e.g. reference voltage, reference current etc.) change at step $k-1$, $P_{grid,k-1}$ and $P_{grid,k-2}$ are the PV inverter output power levels at steps $k-1$ and $k-2$, respectively, C is a constant determining the speed and accuracy of convergence to the MPP point and the function $\text{sign}(x)$ is defined as:

$$\text{sign}(x) = \begin{cases} 1, & \text{if } x \geq 0 \\ -1, & \text{if } x < 0 \end{cases}$$

(8)

The proposed method does not increase the PV inverter cost, since the sensors and signal conditioning circuits required to measure P_{grid} and V_{pv} are also installed in the PV inverter control unit in order to implement the conventional control schemes of the PV inverters.

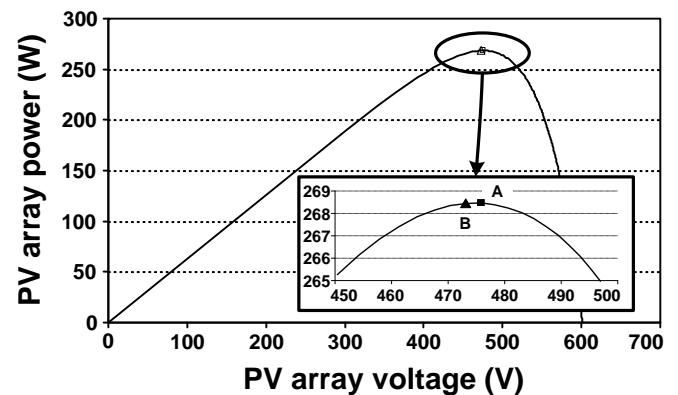


Fig. 5. The power-voltage characteristic of a PV array for MPPT operation.

3. Design examples

The PV inverter design optimization methodology presented in Section 2 has been applied for the optimal design of a single-phase,

full-bridge grid-connected SPWM PV inverter (Fig. 6) comprised of IGBT-type power switches with anti-parallel diodes and an LCL-type output filter. The PV inverter nominal output power and voltage ratings are $P_n = 2000$ W and $V_n = 220$ V, respectively. The PV inverter is connected to a PV array composed of 12 PV modules connected in series. The MPP power and voltage ratings of each PV module, under standard test conditions (STC), are 175W and 35.4V, respectively. The optimization problem design (decision) variables considered during the GA optimal sizing procedure are the PV inverter switching frequency and the LCL output filter components values. Thus, each GA consists of four genes in the form: $X = [L|L_g|C_f|f_s]$. After the GA-based optimization process has been accomplished, the optimal value of the LCL filter damping resistor, R_{dr} , is calculated using the resulting optimal values of L , L_g and C_f , as analyzed in [25]. The PV inverter maintenance cost has not been considered in this design example. The values of P_{cond} and P_{sw} have been calculated using the power loss model presented in [26].

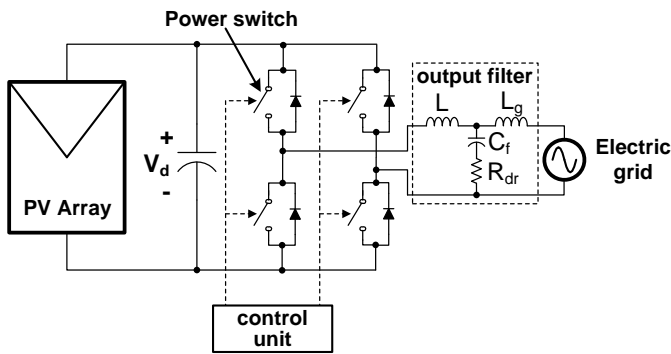


Fig. 6. The block diagram of a grid-connected, single-phase full-bridge PV inverter with an LCL-type output filter.

Since the power switches of the PV inverter under consideration are controlled according to the Sinusoidal Pulse Width Modulation (SPWM) principle [27], the PV inverter switching frequency, f_s (Hz) is constrained to be an integer multiple of the grid frequency, f (Hz). Additionally, the maximum possible value of f_s is dictated by the maximum switching speed

capability of the power switches, $f_{s,max}$ (Hz), specified by their manufacturer:

$$f_s \leq f_{s,max} \quad (9)$$

The LCL-type output filter components values are calculated by the optimization algorithm such that the current ripple at the PV inverter output is below the maximum permissible limit, which is imposed by the grid regulations and standards, as analyzed in [25].

The proposed optimal design method has been implemented in the form of a properly developed software program operating under the MATLAB platform. The Genetic Algorithm functions available in the MATLAB Global Optimization Toolbox have been used in order to derive the global minimum of the PV inverter *LCOE* (objective) function. In order to demonstrate an example of the optimization problem search-space, the variation of the yearly energy injected into the grid, the PV inverter total cost and the *LCOE* for various values of the decision variables L and f_s , in case that the PV inverter is installed in Athens (Greece) and $L_g = 153.6\mu\text{H}$ and $C_f = 6.570\mu\text{F}$, are displayed in Fig. 7. The yearly energy injected into the grid, the PV inverter total cost and the *LCOE* for various values of the decision variables L_g and C_f , in case that the PV inverter is installed in Athens (Greece) and $L = 1.418\text{mH}$ and $f_s = 29.95\text{kHz}$, are illustrated in Fig. 8. The diagrams presented in Figs. 7 and 8 have been constructed using only the values of L , L_g , C_f and f_s which satisfy the optimization problem constraints. It is observed that the *LCOE* function is highly non-linear, thus dictating the use of a computationally efficient optimization algorithm, such as GAs, in order to derive the global optimum values of L , L_g , C_f and f_s which minimize the value of *LCOE*.

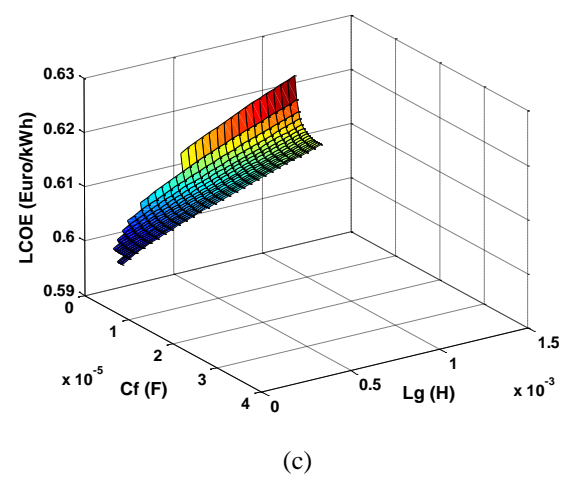
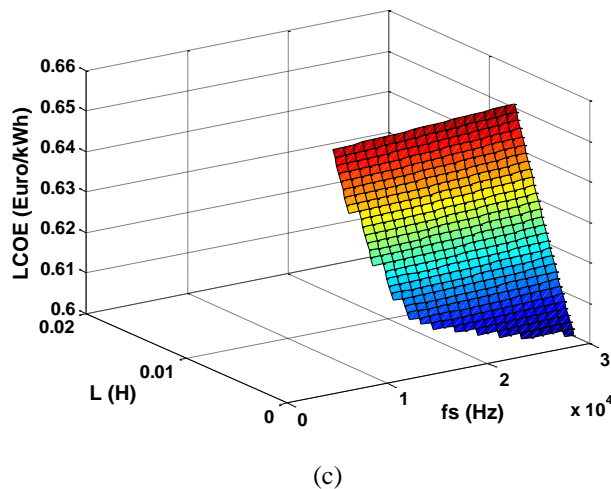
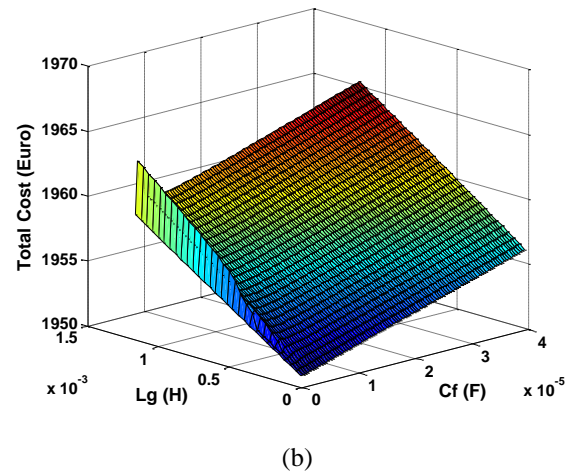
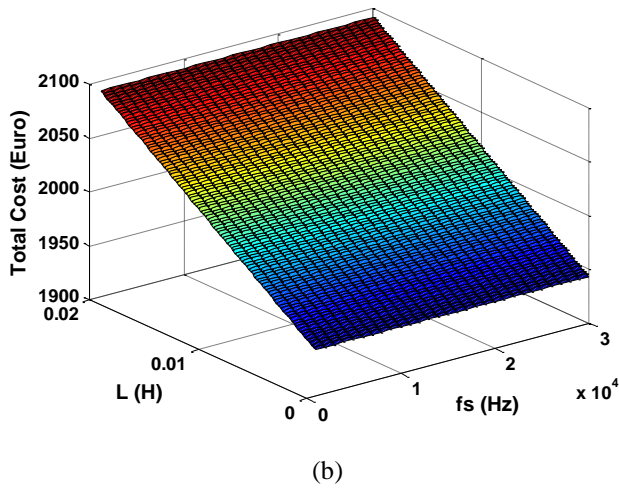
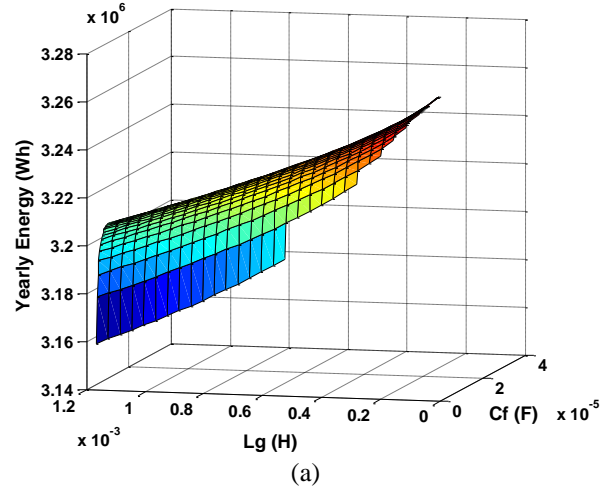
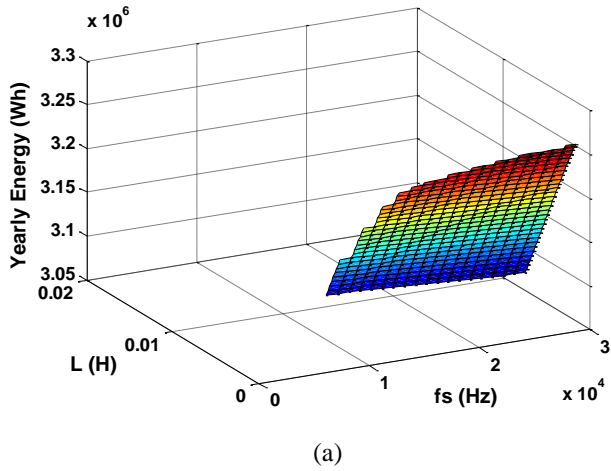


Fig. 7. The yearly energy injected into the grid (a), the PV inverter total cost (b) and the $LCOE$ (c) for various values of the decision variables L and f_s , in case that the PV inverter is installed in Athens (Greece) and $L_g = 153.6\mu\text{H}$ and $C_f = 6.570\mu\text{F}$.

Fig. 8. The yearly energy injected into the grid (a), the PV inverter total cost (b) and the $LCOE$ (c) for various values of the decision variables L_g and C_f , in case that the PV inverter is installed in Athens (Greece) and $L = 1.418\text{mH}$ and $f_s = 29.95\text{kHz}$.

For the application example presented in Figs. 7 and 8, the $LCOE$ is minimized for $L = 1.418\text{mH}$, $L_g = 153.6\mu\text{H}$, $C_f = 6.570\mu\text{F}$ and $f_s = 29.95\text{kHz}$, resulting in $LCOE = 0.6\text{€}/\text{kWh}$, $C_t = 1952.9\text{€}$ and $E_t = 3.255\text{MWh}$. The proposed method has also been applied for the optimal design of PV inverters installed in Murcia (Spain) and Freiburg (Germany). A different set of optimal values of the PV inverter output filter components values is derived in each case, since each of these sites is characterized by a different solar irradiation potential. Additionally, the resulting optimal $LCOE$ values differ by -11.5% (Murcia, Spain) and +45% (Freiburg, Germany), respectively, compared to the optimal $LCOE$ of the PV inverter installed in Athens (Greece). These results indicate the geographical variability of the PV inverter components optimal values, which achieve the optimal (minimum) $LCOE$ for each installation site.

In order to evaluate the performance of the proposed MPPT method, the operation of a commercially available PV inverter with galvanic isolation and a transformerless PV inverter has been simulated using a properly developed software program operating under the MATLAB platform. The power conversion efficiency and MPP voltage range specifications provided by the manufacturer of these PV inverters have been incorporated in the simulation algorithm. The increment of the hourly energy injected into the grid, which is achieved using the proposed MPPT method compared to the injected energy using the conventional MPPT methods, during the same winter day at various sites in Europe for the two PV inverters under study, is presented in Fig. 9. Each of these sites is characterized by a different solar irradiation potential. It is observed that the energy gain is increased when the solar irradiance incident on the PV array is low (e.g. during the sunrise and sunset hours), where both PV inverters operate at low DC input power levels.

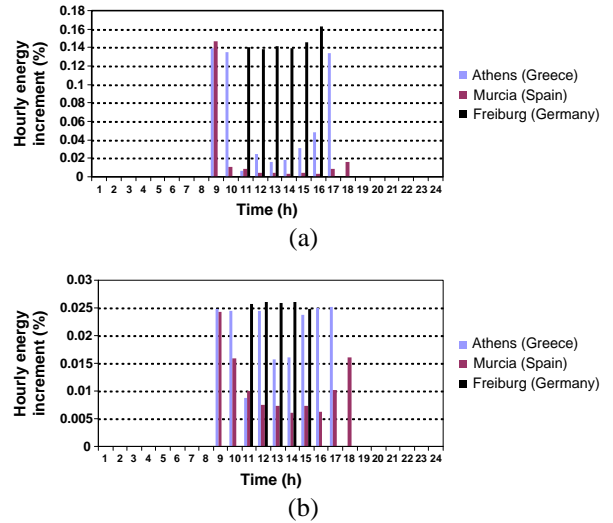


Fig. 9. The increment of the hourly energy injected into the grid by applying the proposed MPPT method during a winter day at various sites in Europe for: (a) a PV inverter with galvanic isolation and (b) a transformerless PV inverter.

Compared to the PV inverter with galvanic isolation [Fig. 9(a)], the energy increment is lower in case of the transformerless PV inverter [Fig. 9(b)], since its power conversion efficiency is less dependent on the operating DC input voltage value. The variation of the voltage deviation between the MPP points of the proposed and the conventional MPPT methods (i.e. points A and B in Fig. 5) during the same winter day at various sites in Europe, is illustrated in Fig. 10.

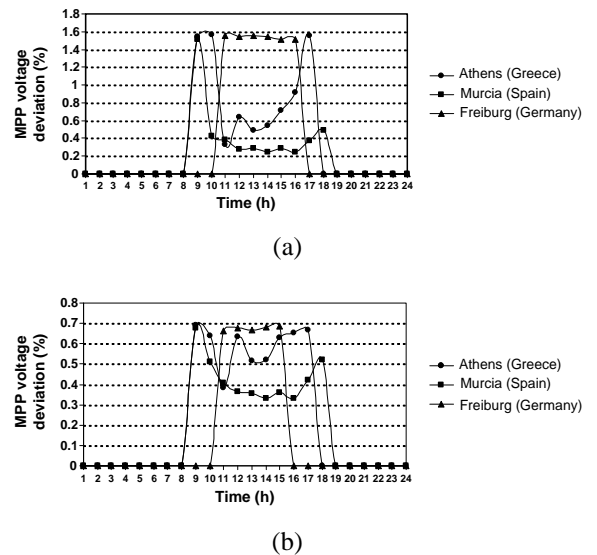


Fig. 10. The voltage deviation between the MPP points of the proposed and the conventional MPPT methods during a winter day at various sites in Europe for: (a) a PV inverter with galvanic isolation and (b) a transformerless PV inverter.

The minimum voltage deviation, developed in case of a PV inverter with galvanic isolation, is 0.25%. In case that a digital PWM generator is used in the PV inverter control unit, this voltage deviation corresponds to a 9-bit resolution of the PV inverter PWM control signal.

4. Conclusions

The energy injected into the electric grid by a PV installation depends on the amount of power extracted from the PV power source and the efficient processing of this power by the DC/AC inverter. In this paper, two new techniques are presented for the optimal design of a PV inverter power section, output filter and MPPT control strategy. The influences of the electric grid regulations and standards as well as the PV array operational characteristics on the design of grid-connected PV inverters have been considered. The proposed methods have been applied for the optimal design of PV inverters installed at various sites in Europe. The simulation results indicate that the optimal values of the PV inverter design (decision) variables depend on the PV inverter specifications (i.e. power rating, nominal output voltage etc.), the technical and economic characteristics of the components used to build the PV inverter and the meteorological conditions prevailing at the installation area. The simultaneous application of these methods for the design of a PV inverter enables the maximization of the PV energy injected into the electric grid by the optimized PV installation, thereby increasing the earnings achieved by the installed PV capacity.

References

- [1] T. Kerekes, R. Teodorescu, P. Rodríguez, G. Vázquez, E. Aldabas, "A new high-efficiency single-phase transformerless PV inverter topology", *IEEE Transactions on Industrial Electronics*, Vol. 58, No. 1, pp. 184-191, January 2011.
- [2] S. Vasconcelos Araújo, P. Zacharias, R. Mallwitz, "Highly efficient single-phase transformerless inverters for grid-connected photovoltaic systems", *IEEE Transactions on Industrial Electronics*, Vol. 57, No. 9, pp. 3118-3128, 2010.
- [3] G. Vazquez, T. Kerekes, A. Rolan, D. Aguilar, A. Luna, G. Azevedo, "Losses and CMV evaluation in transformerless grid-connected PV topologies", *IEEE International Symposium on Industrial Electronics*, pp. 544-548, 2009.
- [4] Huafeng Xiao, Shaojun Xie, Yang Chen, Ruhai Huang, "An optimized transformerless photovoltaic grid-connected inverter", *IEEE Transactions on Industrial Electronics*, Vol. 58, No. 5, pp. 1887-1895, 2011.
- [5] F. Blaabjerg, F. Iov, T. Kerekes, R. Teodorescu, "Trends in power electronics and control of renewable energy systems", *14th International Power Electronics and Motion Control Conference (EPE/PEMC)*, pp. 1-19, 2010.
- [6] E. Figueres, G. Garcera, J. Sandia, F. Gonzalez-Espin, J.C. Rubio, "Sensitivity study of the dynamics of three-phase photovoltaic inverters with an LCL grid filter", *IEEE Transactions on Industrial Electronics*, Vol. 56, No. 3, pp. 706-717, 2009.
- [7] J.M. Guerrero, F. Blaabjerg, T. Zhelev, K. Hemmes, E. Monmasson, S. Jemei, M.P. Comech, R. Granadino, J.I. Frau, "Distributed Generation: toward a new energy paradigm", *IEEE Industrial Electronics Magazine*, Vol. 4, Issue 1, pp. 52-64, 2010.
- [8] C. Cecati, F. Ciancetta, P. Siano, "A multilevel inverter for photovoltaic systems with fuzzy logic control", *IEEE Transactions on Industrial Electronics*, Vol. 57, No. 12, pp. 4115-4125, December 2010.
- [9] H. Patel, V. Agarwal, "MPPT scheme for a PV-fed single-phase single-stage grid-connected inverter operating in CCM with only one current sensor", *IEEE Transactions on Energy Conversion*, Vol. 24, No. 1, pp. 256-263, 2009.
- [10] D. Floricau, G. Gateau, A. Leredde, R. Teodorescu, "The efficiency of three-level active NPC converter for different PWM strategies", *13th European Conference on Power Electronics and Applications*, pp. 1-9, 2009.
- [11] L. Ma, X. Jin, T. Kerekes, M. Liserre, R. Teodorescu, P. Rodriguez, "The PWM strategies of grid-connected distributed generation active NPC inverters", *IEEE Energy Conversion Congress and Exposition (ECCE '09)*, pp. 920-927, 2009.
- [12] N.A. Rahim, J. Selvaraj, "Multistring five-level inverter with novel PWM control scheme for PV application", *IEEE Transactions on Industrial Electronics*, Vol. 57, No. 6, pp. 2111-2123, 2010.
- [13] S.R. Pulikanti, M.S.A. Dahidah, V.G. Agelidis, "SHE-PWM switching strategies for active neutral point clamped multilevel converters", *Australasian Universities Power Engineering Conference*, pp. 1-7, 2008.

- [14] S.B. Kjaer, J.K. Pedersen, F. Blaabjerg, "A review of single-phase grid-connected inverters for photovoltaic modules", *IEEE Transactions on Industry Applications*, Vol. 41, No. 5, pp. 1292-1306, September 2005.
- [15] B. Giesler, "String vs. Central inverters: Dimension of the inverter", *Photon's 1st PV Inverter Conference*, Stuttgart, Germany, pp. 1-23, April 2010.
- [16] S. Balachandran, F.C.Y. Lee, "Algorithms for power converter design optimization", *IEEE Transactions on Aerospace and Electronic Systems*, Vol. 17, No. 3, pp. 422-432, May 1981.
- [17] E. Koutroulis, F. Blaabjerg, "Design optimization of grid-connected PV inverters", *26th Annual IEEE Applied Power Electronics Conference and Exposition*, pp. 691-698, 2011.
- [18] J. Biela, U. Badstuebner, J.W. Kolar, "Design of a 5-kW, 1-U, 10-kW/dm³ resonant DC-DC converter for telecom applications", *IEEE Transactions on Power Electronics*, Vol. 24, No. 7, pp. 1701-1710, July 2009.
- [19] T.C. Neugebauer, D.J. Perreault, "Computer-aided optimization of DC/DC converters for automotive applications", *IEEE Transactions on Power Electronics*, Vol. 18, No. 3, pp. 775-783, May 2003.
- [20] A. Parayandeh, C. Pang, A. Prodic, "Digitally controlled low-power DC-DC converter with instantaneous on-line efficiency optimization", *24th Annual IEEE Applied Power Electronics Conference and Exposition*, pp. 159-163, 2009.
- [21] M. Campbell, J. Blunden, E. Smeloff, P. Aschenbrenner, "Minimizing utility-scale PV power plant LCOE through the use of high capacity factor configurations", *34th IEEE Photovoltaic Specialists Conference*, pp. 421-426, 2009.
- [22] A. Ristow, M. Begovic, A. Pregelj, A. Rohatgi, "Development of a Methodology for Improving Photovoltaic Inverter Reliability", *IEEE Transactions on Industrial Electronics*, Vol. 55, No. 7, pp. 2581-2592, 2008.
- [23] E. Lorenzo, *Solar electricity - Engineering of photovoltaic systems*, 1st ed., Progensa, 1994.
- [24] T. Kerekes, R. Teodorescu, M. Liserre, R. Mastromauro, A. Dell'Aquila, "MPPT algorithm for voltage controlled PV inverters", *11th International Conference on Optimization of Electrical and Electronic Equipment (OPTIM '08)*, pp. 427-432, 2008.
- [25] M. Liserre, F. Blaabjerg, S. Hansen, "Design and control of an LCL-filter-based three-phase active rectifier", *IEEE Transactions on Industry Applications*, Vol. 41, No. 5, pp. 1281-1291, 2005.
- [26] Sushant Kumar Pattnaik, K.K. Mahapatra, "Power loss estimation for PWM and soft-switching inverter using RDCLI", *International MultiConference of Engineers and Computer Scientists*, pp. 1401-1406, 2010.
- [27] Chee Lim Nge, O.-M. Midtgard, L. Norum, T.O. Saetre, "Power loss analysis for single phase grid-connected PV inverters", *31st International Telecommunications Energy Conference*, pp. 1-5, 2009.